Exome Sequencing and *cis*-Regulatory Mapping Identify Mutations in *MAK*, a Gene Encoding a Regulator of Ciliary Length, as a Cause of Retinitis Pigmentosa

Rıza Köksal Özgül,[1,10] Anna M. Siemiatkowska,[2,3,10] Didem Yücel,[1,10] Connie A. Myers,[4] Rob W.J. Collin,[2,3,5] Marijke N. Zonneveld,[2,3] Avigail Beryozkin,[6] Eyal Banin,[6] Carel B. Hoyng,[5] L. Ingeborgh van den Born,[7] The European Retinal Disease Consortium,[9] Ron Bose,[8] Wei Shen,[8] Dror Sharon,[6] Frans P.M. Cremers,[2,3] B. Jeroen Klevering,[5] Anneke I. den Hollander,[2,3,5,*] and Joseph C. Corbo[4,*]

A fundamental challenge in analyzing exome-sequence data is distinguishing pathogenic mutations from background polymorphisms. To address this problem in the context of a genetically heterogeneous disease, retinitis pigmentosa (RP), we devised a candidate-gene prioritization strategy called *cis*-regulatory mapping that utilizes ChIP-seq data for the photoreceptor transcription factor CRX to rank candidate genes. Exome sequencing combined with this approach identified a homozygous nonsense mutation in *male germ cell-associated kinase* (*MAK*) in the single affected member of a consanguineous Turkish family with RP. *MAK* encodes a cilium-associated mitogen-activated protein kinase whose function is conserved from the ciliated alga, *Chlamydomonas reinhardtii,* to humans. Mutations in *MAK* orthologs in mice and other model organisms result in abnormally long cilia and, in mice, rapid photoreceptor degeneration. Subsequent sequence analyses of additional individuals with RP identified five probands with missense mutations in *MAK*. Two of these mutations alter amino acids that are conserved in all known kinases, and an in vitro kinase assay indicates that these mutations result in a loss of kinase activity. Thus, kinase activity appears to be critical for MAK function in humans. This study highlights a previously underappreciated role for CRX as a direct transcriptional regulator of ciliary genes in photoreceptors. In addition, it demonstrates the effectiveness of CRX-based *cis*-regulatory mapping in prioritizing candidate genes from exome data and suggests that this strategy should be generally applicable to a range of retinal diseases.

Introduction

Next-generation sequencing is currently revolutionizing Mendelian disease analysis.[1] It is now possible to identify causative mutations in Mendelian disorders via whole-genome exon (exome) sequencing of affected individuals.[2–5] Yet, given that every human genome contains thousands of codon-altering sequence variants, the fundamental challenge in analyzing exome data is identifying the causal mutation amidst a sea of benign polymorphisms.[1] A first step in sifting through exome-sequence variants is removing those that represent known polymorphisms in the human population. If a disease is thought to be genetically homogeneous, the candidate list can then be further reduced by intersecting exome-sequencing data from multiple affected individuals and different families. In diseases that are genetically heterogeneous, however, this latter filter cannot be applied, and thus there is a need for additional approaches to candidate-gene prioritization.

Retinal degenerations (RD) represent a genetically heterogeneous group of inherited diseases that affect millions of people worldwide.[6–8] Identifying the disease-causing mutation in these individuals is a prerequisite for proper genetic counseling and for the selection of subjects for novel gene-specific therapies. Mutations in over 200 genes have been implicated in RD, and this makes it one of the most genetically heterogeneous families of disease (see RetNet under Web Resources). Despite this growing knowledge base, sequencing of genes known to be mutated in RD locates the causative mutation in only about half of all individuals with RD.[7] Thus, there is a pressing need for new approaches that will accelerate the discovery of additional genes involved in this disease.

Here, we present a general approach to prioritizing retinal-disease gene candidates; we call this approach "*cis*-regulatory mapping." The strategy is based on the findings of a recent study in which we used chromatin immunoprecipitation followed by massively parallel sequencing (ChIP-seq) to identify binding sites for the transcription factor CRX (MIM 602225) across the mouse genome.[9] CRX is a key photoreceptor transcription factor required for the expression of many rod and cone genes,

[1]Institute of Child Health and Metabolism Unit, Department of Pediatrics, Hacettepe University, Ankara 06100, Turkey; [2]Department of Human Genetics, Radboud University Nijmegen Medical Centre, 6500 HC Nijmegen, The Netherlands; [3]Nijmegen Centre for Molecular Life Sciences, Radboud University Nijmegen Medical Centre, 6500 HC Nijmegen, The Netherlands; [4]Department of Pathology and Immunology, Washington University School of Medicine, St. Louis, MO 63110, USA; [5]Department of Ophthalmology, Radboud University Nijmegen Medical Centre, 6500 HC Nijmegen, The Netherlands; [6]Department of Ophthalmology, Hadassah-Hebrew University Medical Center, Jerusalem 91120, Israel; [7]The Rotterdam Eye Hospital, 3011 BH Rotterdam, The Netherlands; [8]Division of Oncology, Department of Medicine, Washington University School of Medicine, St. Louis, MO 63110, USA
[9]Full list of authors in Acknowledgements
[10]These authors contributed equally
*Correspondence: a.denhollander@antrg.umcn.nl (A.I.d.H.), jcorbo@pathology.wustl.edu (J.C.C.)
DOI 10.1016/j.ajhg.2011.07.005.

including the majority of genes known to be mutated in RD.[10–13] CRX directly regulates photoreceptor genes by binding to ~10,000 *cis*-regulatory regions referred to as CRX-bound regions (CBRs).[9] Because the majority of genes involved in RD are preferentially expressed in photoreceptors,[9,11,14] we reasoned that clustering of CBRs could be used to pinpoint genes with mutations causing RD within lists of candidate genes.

We applied the combined strategy of exome sequencing and prioritization of candidate genes by CBR clustering to a Turkish subject with retinitis pigmentosa (RP) who is the only affected member of a consanguineous family. This analysis resulted in the identification of a homozygous nonsense mutation in *male germ cell-associated kinase* (*MAK*; MIM 154235). We subsequently screened Dutch and Israeli subjects with RP and found five additional missense mutations affecting critical residues of this protein. *MAK* encodes a highly-conserved mitogen-activated protein (MAP) kinase that regulates ciliary length in a wide range of species.[15–17] In addition, it has recently been shown that *Mak* mutations in mice cause rapid photoreceptor degeneration.[17] This study demonstrates the utility of CRX-based *cis*-regulatory mapping as an approach for prioritizing candidate genes from whole-exome data in individuals with RD.

Subjects and Methods

cis-Regulatory Mapping

CRX ChIP-seq data were generated from 8-week-old mouse retinas as previously described.[9] We used the UCSC Genome Browser liftover tool to map mouse CBRs onto the human genome.[18] CBRs were then assigned to individual genes as previously described.[9] CBRs were assigned to a total of 21,515 and 21,912 RefSeq genes in humans and mice, respectively (Table S1, available online). This same procedure was repeated for CRX ChIP-seq data generated from 8-week-old $Nrl^{-/-}$ mouse retinas.[9] Lists of candidate genes derived from defined genomic regions or exome-sequencing datasets were numerically ranked according to their raw read counts as given in Table S1.

Families and DNA Extraction

The tenets of the Declaration of Helsinki were followed, and informed consent was obtained prior to donation of a blood sample from all individuals who participated in this study. Blood samples for DNA analysis were obtained from affected and unaffected family members. Genomic DNA was extracted from peripheral blood samples with the FlexiGene DNA kit (Qiagen, Venlo, the Netherlands) or with a standard salting-out procedure.[19] The ethical review boards of Radboud University Nijmegen Medical Centre, Hacettepe University, and Hadassah-Hebrew University Medical Center approved this study.

Clinical Evaluation

Ophthalmic examinations, including electroretinography (ERG) according to International Society for Clinical Electrophysiology of Vision (ISCEV) standards and fundus photography, were performed for all affected individuals. Goldmann perimetry was performed in seven of the eight affected individuals.

Exome Sequencing and Analysis

Five micrograms of high-quality genomic DNA from subject RP-2011 was prepared for sequencing with an Illumina Paired-End Sample Preparation kit (Illumina Inc., San Diego, CA, USA) according to manufacturer's instructions. Coding exons were captured from the resultant sample with the Agilent SureSelect Human All Exon kit (Agilent Technologies, Santa Clara, CA, USA) according to manufacturer's instructions. Cluster generation was performed with the Paired-End Cluster Generation kit (v2) and the Illumina Cluster Station. A paired-end, 75 bp run was performed on an Illumina Genome Analyzer IIx. Images were analyzed with the standard Illumina Pipeline (version 1.4), and a total of 4.5 billion bases of sequence were obtained. Sequences were aligned with the human genome reference sequence (build hg18), and variant calls were made and annotated according to the dbSNP database (build 129). A total of 52 putative homozygous nucleotide changes not present in the dbSNP database were identified in 38 genes (Table S2). These genes were ranked according to CRX-binding scores, and the top five candidate genes were further evaluated by direct sequence analysis.

Homozygosity Mapping and Mutation Analysis

Whole-genome SNP analysis was performed on subject RP-2011, her parents, and her siblings with the Affymetrix GeneChip Mapping 250K array set (Affymetrix, Santa Clara, CA, USA). Homozygous regions were calculated with Affymetrix GTYPE software and the VIGENOS (Visual Genome Studio) Program (Hemosoft Inc., Ankara, Turkey). In addition, whole-genome SNP analysis was performed on 334 subjects of Dutch, Italian, Israeli, and Palestinian origin with the Illumina 6K or the Affymetrix 10K, 250K, 5.0, or 6.0 SNP arrays (SNP analysis of Dutch subjects was reported previously[20]). Homozygous regions were calculated with Partek software (Partek Incorporated, St. Louis, MO, USA) or PLINK software.[21]

Primers for PCR amplification of the 15 exons and exon-intron boundaries of *MAK* (including the retina-enriched alternative exon 13) were designed with Primer 3 software (Table S3). PCR was performed with 50 ng of genomic DNA in 25 μl reactions for 35 cycles. PCR fragments were purified with 96-well PCR filter plates (Millipore, Billerica, MA, USA), and mutation analysis was performed by direct sequencing of purified PCR products.

Animal Studies

Adult CD1 mice were housed at Washington University in St. Louis (St. Louis, MO, USA), in an air-conditioned environment on a 12 hr light-dark cycle at 22°C and had free access to water and food. All animal studies were conducted in accordance with the Guide for the Care and Use of Laboratory Animals and the Animal Welfare Act and were approved by the Washington University in St. Louis institutional animal care and use committee (approval number 20110089).

CBR-Reporter Fusion Constructs

Three CBRs identified around the *MAK* locus were obtained by PCR from human genomic DNA with the primer pairs indicated in Table S3. The resultant PCR products were cloned into the *Rho*-basal DsRed reporter vector with the restriction enzyme sites underlined in the primer (Table S3).[13] Retinal

electroporation and explant cultures were performed exactly as described previously.[13]

MAK Expression Constructs

Human retinal cDNA was generated from total human retinal RNA with SuperScript II reverse transcriptase (Invitrogen, Carlsbad, CA, USA) per the manufacturer's instructions. The retinal isoform of *MAK* was generated by PCR with primers shown in Table S3. A Kozak consensus site (upper case letters in Table S3) was added to the 5′ primer. The resultant PCR product was digested with *Sac*II and *Not*I, (underlined in primers in Table S3) and cloned into an intermediate cloning vector. We determined by sequencing that the clone was free of mutations and contained the retina-enriched exon 13. *MAK* mutations were generated by site directed mutagenesis with the Quik-Change II kit (Stratagene, Cedar Creek, TX, USA) according to the manufacturer's instructions. Wild-type and mutant forms of the *MAK* expression construct were then cloned in frame with the C-terminal Myc/his tag in pcDNA3.1(+)Myc/his A vector (Invitrogen).

In Vitro Kinase Assay

MAK-WT-Myc/his, MAK-mut-Myc/his, or empty vector was transfected into HEK293 (PlatE) cells with TransIT-LT1 transfection reagent (Mirus Bio LLC, Madison, WI, USA). Forty-eight hours after transfection the cells were washed twice with cold PBS and lysed on plate in modified RIPA buffer (150 mM NaCl, 50 mM Tris [pH 7.4], 1% NP-40, 0.25% Sodium Deoxycholate, 1 mM EDTA). Expression of MAK was confirmed via immunoblot analysis with 40 μg of total protein from the immunoprecipitation input lysate. Proteins were run on a 4-12% Bis-Tris gel (Invitrogen) and transferred to a Protran nitrocellulose membrane (Sigma, St. Louis, MO). The membranes were blocked for 1 hour at room temperature with 5% nonfat dry milk in TBST (Tris-buffered saline with 0.1% Tween 20), incubated with 1:500 dilution of mouse monoclonal c-Myc (9E10) (Santa Cruz Biotechnology, Santa Cruz, CA) in TBST with 5% nonfat dry milk followed by 1:5000 dilution of ImmunoPure Goat anti-Mouse HRP (Thermo Scientific Pierce Protein Research Products, Rockford, IL) and signal was detected on Classic Blue autoradiography film (Molecular Technologies, St. Louis, MO) via chemiluminescence with Immun-Star WesternC (Bio-Rad Hercules, CA) following the manufacturer's instructions.

For the kinase assay, cleared lysate was rotated with anti-c-Myc Agarose beads (Sigma, St. Louis, MO) for 3 hrs at 4°C. Beads were washed 4 times with RIPA buffer and then twice in kinase equilibration buffer (20 mM HEPES pH 7.5, 10 mM MgCl2, 1 mM DTT). Beads were resuspended in 20 μl of kinase assay buffer (20 mM HEPES [pH 7.5], 10 mM $MgCl_2$, 1 mM DTT, 10 mM $MnCl_2$, 2 μg/ml leupeptin, 10 μM ATP, 2 μg myelin basic protein [Active Motif, Carlsbad, CA], and 2 μCi ATP-γ ^{32}P) and incubated for 30 min at 30°C. Reactions were terminated with 5× SDS PAGE buffer and run on a 15% SDS-PAGE gel. The dried gels were exposed to a Phosphorimager screen overnight and scanned with a Typhoon Phosphorimager (GE Healthcare, Piscataway, NJ). Quantitation of scans was performed with ImageJ software.

Analysis of *MAK* Isoforms

We used Trizol (Invitrogen) or Paxgene Blood RNA kit (Qiagen, Venlo, the Netherlands) to isolate RNA from fresh human retina and testis according to the manufacturer's instructions. We used SuperScript II reverse transcriptase (Invitrogen) or iScript cDNA Synthesis kit (BioRad, Hercules, CA, USA) to generate cDNA per the manufacturer's instructions and PCR primers that span the 75 bp alternative exon to amplify MAK transcripts from retinal and testis cDNA (Table S3).

Bioinformatic Analysis of Ciliary-Gene Regulation by CRX

A list of 200 phylogenetically conserved ciliary genes with RefSeq identifiers was obtained from Table S8 of a recent study of the mouse photoreceptor sensory cilium complex[22] and was compared with the genes listed in Table S1 of the present study. All ciliary genes that had assigned CBRs in either the wild-type or $Nrl^{-/-}$ datasets were defined as CBR associated.

Results

CRX-Based *cis*-Regulatory Mapping of Retinal-Disease Genes

The majority of genes known to be involved in RD show photoreceptor-enriched expression;[9,11,14] thus we hypothesized that the genome-wide pattern of binding of CRX, a global transcriptional regulator of photoreceptor genes, could be used to pinpoint novel genes that, when mutated, cause RD. We previously discovered that CBRs cluster around known photoreceptor genes in the mouse.[9] To determine whether this is also true in humans, we used the UCSC Genome Browser liftover tool to map 10,212 mouse CBRs onto the human genome. We found that ~80% (8,214/10,212) of mouse CBRs mapped successfully to the human genome. We assigned CBRs to individual genes across the human genome on the basis of proximity and found that they tightly cluster around photoreceptor genes (Table S1).

Next, we determined whether these assignments could be used to identify retinal-disease genes within defined genomic intervals. As a test case, we attempted to rediscover *Rhodopsin* (*RHO*; MIM 180380) because mutations in this gene are known to cause RP.[23,24] We analyzed a 51 gene region around *RHO* (including 25 on either side of *RHO*; Figure 1A). The CBR assignments in the immediate vicinity of *RHO* are shown in Figure 1B. The number of raw sequence reads at a given CBR reflects the extent of CRX binding at that CBR. Thus, by tallying the number of raw sequence reads assigned to each of the 51 genes in this region, we can derive a ranked list of genes that reflects how heavily they are bound by CRX. With this approach, *RHO* is ranked as the number one retinal-disease gene candidate within this genomic region (Figure 1C).

Next, we attempted to use this approach to rediscover the 33 additional genes known to be mutated in autosomal-recessive RP. As was done with *RHO*, we created ranked lists of candidate genes for a 51 gene region around each locus. We found that in 62% of cases (21/34, including *RHO*), the gene known to be mutated in autosomal-recessive RP ranked among the top three candidates (Figure S1A, available online). In addition, more than one-third (12/34) of the genes mutated in RP were ranked as the

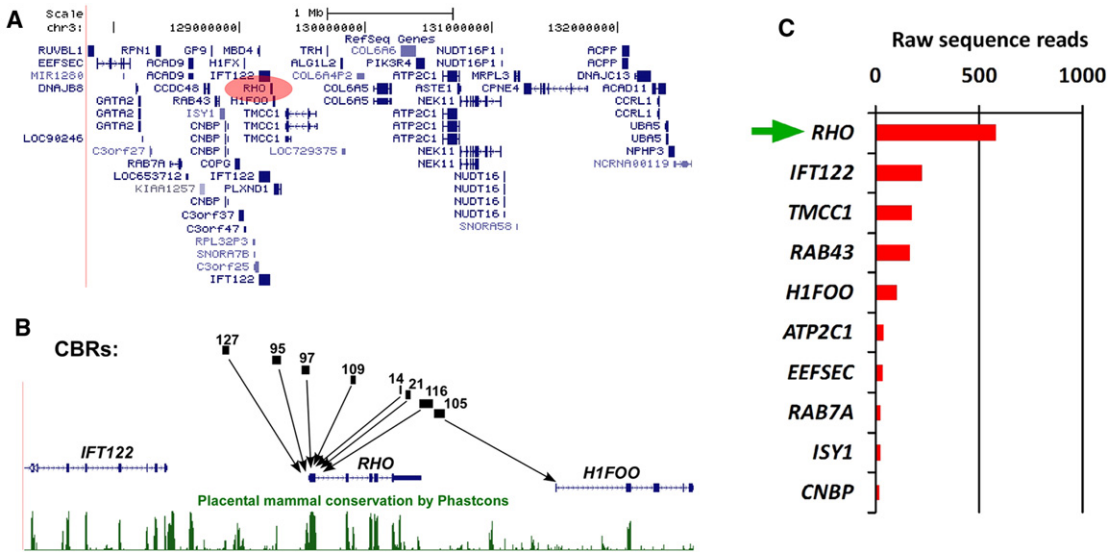

Figure 1. *cis*-Regulatory Mapping at the *RHO* Locus
(A) The genomic interval including 25 genes on either side of the human *RHO* locus (pink oval) spans 4.8 Mb.
(B) There are eight CBRs in the immediate vicinity of the *RHO* locus that were assigned to nearby genes as indicated by the arrows. The number of raw sequence reads corresponding to each of the CBRs is shown.
(C) The 51 genes shown in (A) were ranked according to the number of raw sequence reads assigned to them. The *RHO* locus (green arrow), which was assigned a total of 579 raw sequence reads, ranked number one out of all 51 genes in this interval. Only the ten highest ranking genes are shown. Portions of the images in (A) and (B) are adapted from the UCSC Genome Browser.[38]

number one candidate within their corresponding region. An additional gene (*DHDDS*; MIM 608172) was ranked fifth in its interval. Overall, the *cis*-regulatory mapping approach successfully prioritized the gene known to be mutated in RP in nearly two-thirds of cases.

In 12 cases, CRX-based *cis*-regulatory mapping failed to rank the known gene highly. The reason for this becomes apparent upon inspection of the expression pattern of these genes. Half of the genes (6/12) are expressed in retinal pigment epithelium (RPE) and not in photoreceptors (Figure S1B). Thus, these genes would not be predicted to be regulatory targets of CRX in the mouse. Another gene that was not assigned any CBRs was *EYS* (MIM 612424). In this case, the approach failed because the mouse genome does not contain an ortholog of *EYS*, and thus no CBRs were found in its vicinity.

This same approach can also be extended to other categories of retinal disease. We found comparable rates of success upon reanalyzing known loci implicated in autosomal-dominant RP, autosomal-recessive Leber congenital amaurosis, and autosomal-dominant cone-rod dystrophy (data not shown). In contrast, this approach was less successful at predicting the genes mutated in achromatopsia, which tend to be cone-specific.[25] Given that the Crx ChIP-seq dataset we used derives from wild-type retinas, and most of the raw sequence reads therefore derive from rods,[9] this failure is understandable. To address this issue, we performed *cis*-regulatory mapping by using Crx ChIP-seq data derived from $Nrl^{-/-}$ retinas that represent an enriched source of cones[9,26–28] (Table S1). When we applied this approach to the known achromatopsia (ACHM) loci, we found that three of the four genes known to be mutated in autosomal-recessive ACHM were predicted as the number one candidate within a 51 gene interval (data not shown).

Mutations in the Ciliary Gene *MAK* Cause Autosomal-Recessive RP

To determine whether CRX-based *cis*-regulatory mapping could help to identify causative genes within exome datasets, we analyzed exome-sequence data from an individual with RP after first excluding mutations in genes known to be implicated in this disease. This Turkish individual, whose parents were first cousins, is the only affected member of her family (IV:1 in Figure 2A). We identified sequence variants in the subject's exome data and removed all variants found in the dbSNP database (build 129), which left a total of 38 genes with putative homozygous or compound heterozygous mutations (Table S2). We then ranked these 38 genes by using CRX-based *cis*-regulatory mapping (Figure 2B and Table S2). The top five candidate mutations were tested by Sanger sequencing, which confirmed homozygous variants in *SGIP1* (MIM 611540), *MAK*, and *FRYL* in the subject. The variants identified in *USH2A* (MIM 608400) and *CTBP2* (MIM 602619) were not confirmed. The exons containing the variants in *SGIP1*, *MAK*, and *FRYL* were then sequenced in the subject's parents and siblings. The variant in *SGIP1* did not segregate with the disease and was therefore excluded from the analysis. The variants in *FRYL* and *MAK* both segregated with the disease phenotype. Homozygosity mapping performed on the subject identified nine regions of identity by descent totaling ~48 Mb of genomic DNA (data not shown). *FRYL* and *MAK* fall within the first and fourth

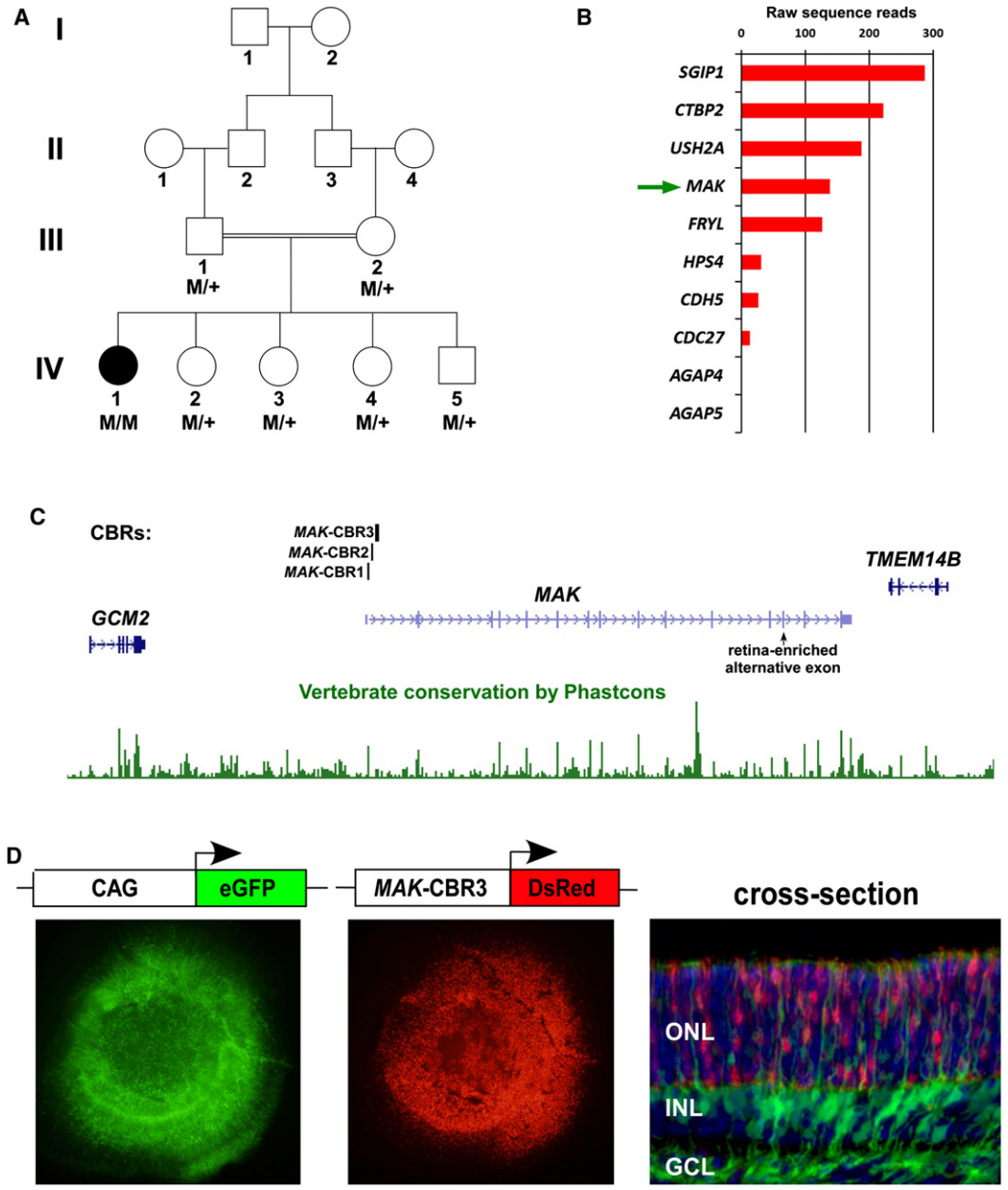

Figure 2. *cis*-Regulatory Mapping Identifies *MAK* as a Cause of Retinitis Pigmentosa
(A) The family tree of the Turkish subject with RP.
(B) The 38 genes with putative homozygous mutations in the exome-sequence dataset were ranked according to their number of raw sequence reads. *MAK* (green arrow) ranked fourth. Only the ten highest ranking genes are shown.
(C) CBRs in the vicinity of the *MAK* locus.
(D) A PCR product encompassing *MAK*-CBR3 was cloned into a DsRed reporter vector and coelectroporated along with a ubiquitously expressing CAG-eGFP loading control into explanted P0 mouse retinas. The retinas were grown for 8 days and then imaged in both red and green channels in flat-mount and as cross-sections. *MAK*-CBR3 drives strong, photoreceptor-specific expression restricted to the outer nuclear layer. The following abbreviations are used: ONL, outer nuclear layer; INL, inner nuclear layer; GCL, ganglion cell layer.

largest identical-by-descent regions, respectively. The amino acid change in *FRYL* (RefSeq NM_015030.1; c.2668C>T [p.Pro890Ser]) is predicted to be nonpathogenic by two prediction programs (SIFT: tolerated, score 0.28; Polyphen2: benign, score 0.015). Given that the mutation in *MAK* (RefSeq NM_001242957.1; c.718C>T [p.Gln240X]) resulted in a premature stop codon predicted to truncate more than half of the protein, we focused our subsequent analysis on this candidate. Both of the subject's parents and her four healthy siblings were all heterozygous carriers of the mutation, which was not identified in 130 healthy Turkish control individuals (Figure 2A).

Three CBRs were identified around the *MAK* locus: *MAK*-CBR1, which partly overlapped the first noncoding exon of *MAK*, and *MAK*-CBR2 and 3, which are located within the first intron (Figure 2C). We tested the

Table 1. Clinical Characteristics of Individuals with *MAK* Mutations

Subject Number	Country of Origin	Gender	Age at Diagnosis (years)	Age at Most Recent Examination	Initial Symptom	Visual Acuity (Refraction in Diopters)		Full Field ERG	Fundoscopic Findings	Perimetry	Additional Findings	Diagnosis	*MAK* Mutation
						Right Eye	Left Eye						
RP-2011	Turkey	F	~20	31	night blindness	20/25 no refraction	20/25 no refraction	minimal responses for both rods and cones	diffuse pigmentation throughout fundus	constricted visual fields; 25 degrees	consanguinity	RP	c.718C>T; (p.Gln240*)/ c.718C>T; (p.Gln240*)
009539	Netherlands	F	37	57	night blindness	20/125 (−2.5 SE)	20/40 (−1.5 SE)	no responses	bone spicules and attenuated vessels; Bullseye-like maculopathy	central islands of 10 degrees with small nasal patches	consanguinity; lens opacities	RP	c.388A>C (p.Asn130His)/ c.388A>C (p.Asn130His)
027775	Netherlands	M	23[a]	23	visual field defects	20/25 (−2.25 SE)	20/25 (−3 SE)	severely reduced rod responses, mildly reduced cone responses	no bone spicules; RPE alterations and possibly early stage atrophy; attenuated vessels; optic disc pallor	constricted visual field, 20 degrees	none	RP	c.37G>A (p.Gly13Ser)/ c.37G>A (p.Gly13Ser)
038230	Netherlands	F	43[b]	47	night blindness (since childhood); visual field defects at presentation	20/20 (−7 SE)	20/20 (−7 SE)	signficantly reduced rod responses and mildly reduced cone responses (at 43 years)	mild pallor optic disc, moderately attenuated vessels; preserved macular region; RPE atrophy and bone-spicules in the nasal quadrants	constricted visual fields with temporal scotomas in the midperiphery	none	sectorial RP	c.79G>C (p.Gly27Arg)/ c.542T>C (p.Ile181Thr)
012115	Netherlands	F	51	59	night blindness	20/32 no refraction	20/100 no refraction	NA	attenuated vessels; bone spicule pigmentation	mild constriction and arcuate scotomas	subcapsular posterior cataract OS>OD	RP	c.79G>A (p.Gly27Arg)/ r.0
MOL07 08-1	Israel	F	32	49	night blindness	20/32 –20/40 (−2.75 SE)	20/25-20/32 (−2.5 SE)	severely reduced rod responses, moderately reduced cone responses	posterior poles normal; mild changes in nasal retina	localized visual field loss: BE midperipheral temporal scotomas	consanguinity	sectorial RP	c.497G>A (p.Arg166His)/ c.497G>A (p.Arg166His)

Table 1. *Continued*

Subject Number	Country of Origin	Gender	Age at Diagnosis (years)	Age at Most Recent Examination	Initial Symptom	Visual Acuity (Refraction in Diopters)		Full Field ERG	Fundoscopic Findings	Perimetry	Additional Findings	Diagnosis	*MAK* Mutation
						Right Eye	Left Eye						
MOL0708-2	Israel	M	25	66	night blindness	20/63 (+0.75 SE)	20/50 (−2.75 SE)	NA	NA	NA	sibling of MOL0708-1	RP	c.497G>A (p.Arg166His)/ c.497G>A (p.Arg166His)
MOL0708-4	Israel	F	30	57	night blindness	20/50 aphakic	20/32 aphakic	severely reduced cone and rod responses	mild pigmentary changes around arcades	midperipheral scotomas, temporal more than nasal	sibling of MOL0708-1; congenital cataract	RP	c.497G>A (p.Arg166His)/ c.497G>A (p.Arg166His)

The following abbreviations are used: F, female; M, male; D, diopters; ERG, electroretinogram; NA, not available; SE, spherical equivalent.
[a]Severe tunnel vision was present at age 23.
[b]Night blindness since childhood.

cis-regulatory activity of these three human CBRs by electroporating individual CBR-reporter fusion constructs into newborn mouse retinas. Whereas *MAK*-CBR1 and 2 did not drive any expression by themselves (data not shown), *MAK*-CBR3 drove strong, photoreceptor-specific expression within the retina (Figure 2D). These findings suggest that *MAK*-CBR3 represents a bona fide *cis*-regulatory region for *MAK* and that CRX is a direct transcriptional regulator of this gene. Previous studies have shown that about half of CBRs demonstrate autonomous photoreceptor-specific *cis*-regulatory activity in this assay.[9,13] In addition, many of the nonfunctioning CBRs can act as potent enhancers or repressors when placed next to an adjacent CBR.[9] We therefore tested *MAK*-CBR1 and 2 for enhancer activity by cloning them upstream of a *Rho* promoter shown previously to drive rod-specific expression.[9] This assay revealed a strong enhancement of reporter transcription relative to the *Rho* promoter alone, indicating that *MAK*-CBR1 and 2 do indeed possess potent enhancer activity (data not shown).

Next, we screened for *MAK* mutations in additional individuals with RP. Whole-genome SNP analysis of 334 isolated or autosomal-recessive RP subjects of Dutch, Italian, Israeli, and Palestinian origins revealed 11 RP probands with a large homozygous region encompassing *MAK* (Table S4). Mutation analysis of *MAK* revealed homozygous missense mutations in three of these probands: c.37G>A (p.Gly13Ser) in subject 027775 (II:3 in Figure S2), c.388A>C (p.Asn130His) in subject 009539 (II:5 in Figure S2), and c.497G>A (p.Arg166His) in subject MOL0708-1 (II:4 in Figure S2) (Table 1). The p.Arg166His mutation segregates with the disease in the family of subject MOL0708-1 (which is of oriental Jewish origin): two affected siblings are homozygous for the mutation, whereas one unaffected sibling is heterozygous and two unaffected siblings do not carry the mutation (Figure S2). The p.Arg166His mutation was identified in the heterozygous state in one out of 217 oriental Jewish controls. The p.Gly13Ser and p.Asn130His mutations were not identified in 163 Dutch control individuals.

In addition, we screened 93 Dutch isolated or autosomal-recessive RP subjects for mutations in all coding exons and splice junctions of *MAK* by direct sequencing. In the majority of these individuals, mutations in genes previously implicated in RP had already been excluded. This analysis identified compound heterozygous missense mutations in subject 038230 (II:3 in Figure S2): c.79G>C (p.Gly27Arg) and c.542T>C (p.Ile181Thr) (Table 1). Segregation analysis within this family revealed that the sister of this individual carries both of the mutations. The disease status of this individual must be determined through clinical tests. Heterozygous changes were detected in two RP subjects: c.79G>A (p.Gly27Arg) was detected in subject 012115 (II:1 in Figure S2) and c.974C>T (p.Pro325Leu) in subject 050135 (data not shown). Although no second pathogenic allele was found in individual 012115 on the genomic DNA level, RNA analysis of peripheral blood revealed the presence of

a hemizygous c.79G>A (p.Gly27Arg) mutation, indicating the lack of an RNA product from the second allele. The p.Pro325Leu variant in subject 050135 was not detected in the subject's affected sibling, suggesting that it is not pathogenic, when assuming an autosomal-recessive mode of inheritance. None of the missense variants (p.Gly27Arg, p.Ile181Thr, and p.Pro325Leu) were detected in 163 Dutch control individuals.

The clinical findings for individuals carrying *MAK* mutations are presented in Table 1. The age at diagnosis in three of eight subjects was in the third decade of life and in the remaining five subjects in the fourth through sixth decades of life. In retrospect, however, retinal dysfunction had been present at an earlier age in at least one subject (038230). Visual acuity was relatively preserved in the subjects, and six of the eight subjects displayed 20/40 or better in at least one eye. The visual field appears to be more heavily affected: half of the subjects experienced tunnel vision of 25 degrees or less. Interestingly, two subjects demonstrated sectorial RP. Consanguinity was present in at least three of the index subjects. Overall, individuals with *MAK* mutations appear to have a disease course that is somewhat less rapid and severe than what has been observed in a number of other genetic forms of RP.

MAK encodes a highly-conserved regulator of ciliary length that contains a MAP kinase domain in its N-terminal half (Figure 3A). Mutations in the *MAK* orthologs of *Chlamydomonas reinhardtii, Leishmania mexicana, Caenorhabditis elegans*, and mice result in formation of abnormally long cilia.[15–17,29] *Mak* mutations in mice also cause rapid degeneration of photoreceptors.[17] All six of the putatively pathogenic mutations in *MAK* that we identified fall within the conserved kinase domain (Figure 3A). The most severe mutation (p.Gln240*) creates a premature stop codon within the C-terminal portion of the domain that is predicted to remove kinase subdomain XI.[30] All missense mutations (p.Gly13Ser, p.Gly27Arg, p.N130S, p.Arg166His, and p.Ile181Thr) are predicted to be pathogenic with various pathogenicity prediction programs (Table S5). In addition, two missense mutations (p.Gly13Ser and p.Asn130His) affect amino acids that are universally conserved across all known kinases.[30] These amino acids correspond to glycine 52 and asparagine 171 in cAMP-dependent protein kinase that serves as a paradigm for kinase structure/function relations.[30–32] Glycine 52 forms part of a critical glycine-rich loop required for binding ATP.[32] Asparagine 171, in contrast, acts as a stabilizer within the catalytic loop of the protein.[32] The other three mutations we identified (p.Gly27Arg, p.Arg166His, and p.Ile181Thr) all affect highly-conserved residues within the kinase domain. These results strongly suggest that kinase activity is critical for the normal function of the MAK gene product in photoreceptors.

In order to evaluate the effects of these mutations on MAK kinase activity directly, we employed an in vitro kinase assay. An expression construct was engineered that contained the full-length wild-type human *MAK* coding sequence derived from retinal cDNA. In addition, two variant constructs were engineered that carried the human mutations that affect universally conserved amino acids (p.Gly13Ser and p.Asn130His). We found that the wild-type MAK protein resulted in increased phosphorylation of myelin basic protein relative to background (Figure 3B). In contrast, the kinase activity observed with the two mutant forms of MAK was essentially the same as that seen with the empty vector (Figure 3B). These results confirm that these two disease-causing mutations result in a loss of kinase activity in vitro.

PCR amplification of the full-length *MAK* coding sequence from human retina resulted in the identification of a photoreceptor-enriched alternative exon (number 13) that was previously reported in mice[17] (Figure 4A). This exon corresponds to a block of phylogenetic conservation encoding 25 amino acids (Figure 4A). Given the relatively restricted pattern of expression of *MAK* in testis and retina,[17] we determined the extent to which the two transcript isoforms (with and without the alternative exon) are expressed in these two tissues in humans. We found that the longer isoform (including the alternative exon) is the predominant species in the retina, and there is only a barely detectable level of expression of the shorter isoform (Figure 4B). In contrast, in testis, the short isoform predominates, whereas the longer form is detectable at lower levels. A similar pattern of retinal- and testis-predominance of the long and short isoforms, respectively, was also observed in mice (data not shown).

CRX Is a Global Transcriptional Regulator of Ciliary Genes in Photoreceptors

The binding of CRX around the *MAK* locus suggests a previously underappreciated role for CRX in regulating the expression of cilium-related genes in photoreceptors. To explore this idea further, we bioinformatically analyzed a large set of ciliary genes for direct binding by CRX by using our CRX ChIP-seq dataset. A prior analysis of the proteome of the mouse photoreceptor sensory cilium complex (i.e., the outer segment) revealed the presence of more than a thousand different proteins in this structure.[22] Among these were more than 200 genes encoding phylogenetically conserved ciliary proteins. We analyzed 200 of these genes and found that ~60% (119/200) had CBRs associated with them (data not shown). This figure represents a marked enrichment for CRX binding around ciliary genes compared to binding around all genes in the genome ($P = 1.07 \times 10^{-24}$, hypergeometric distribution). CRX binding was also detected in the proximal promoter region of *RFX1* (MIM 600006), a key transcriptional regulator of ciliary genes (data not shown).[33] Taken together, these data suggest that CRX might directly regulate many cilium-related genes including a critical transcriptional regulator of these genes.

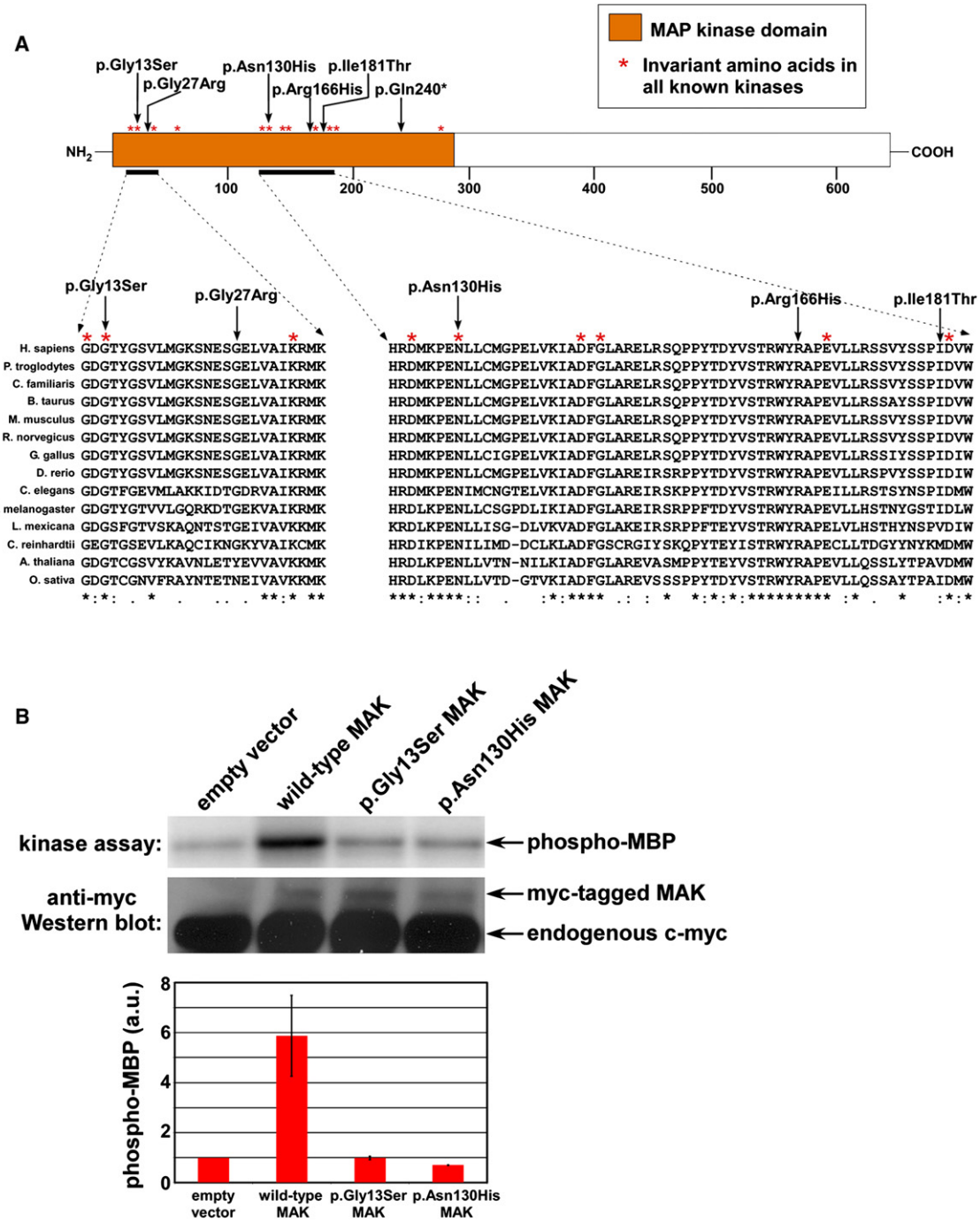

Figure 3. Analysis of Additional *MAK* Mutations

(A) Schematic of the MAK protein shows the location of six identified disease-associated mutations. Cross-species comparison of two regions of MAK indicate that all the identified missense mutations affect highly-conserved residues.

(B) In vitro kinase assay showing that two mutations in MAK, p.Gly13Ser and p.Asn130His, result in a loss of kinase activity. Note that there is a modest background level of phosphorylation of myelin basic protein (MBP) even in the empty vector control condition. The graph at the bottom shows results for two biological replicates of the kinase assay. The amount of phospho-MBP is normalized to the amount of kinase expressed. Error bars represent standard deviation.

Discussion

This study introduces a bioinformatic strategy called *cis*-regulatory mapping for prioritizing candidate genes within lists derived from either genetic mapping or exome sequencing of individuals with retinal degeneration. We used this approach to identify a homozygous mutation in *MAK* in a Turkish individual with RP. Further studies revealed additional mutations in *MAK* in RP subjects from several geographical regions. *MAK* encodes a cilium-associated MAP kinase that is selectively expressed in retina and testis. Two disease-causing mutations in *MAK*

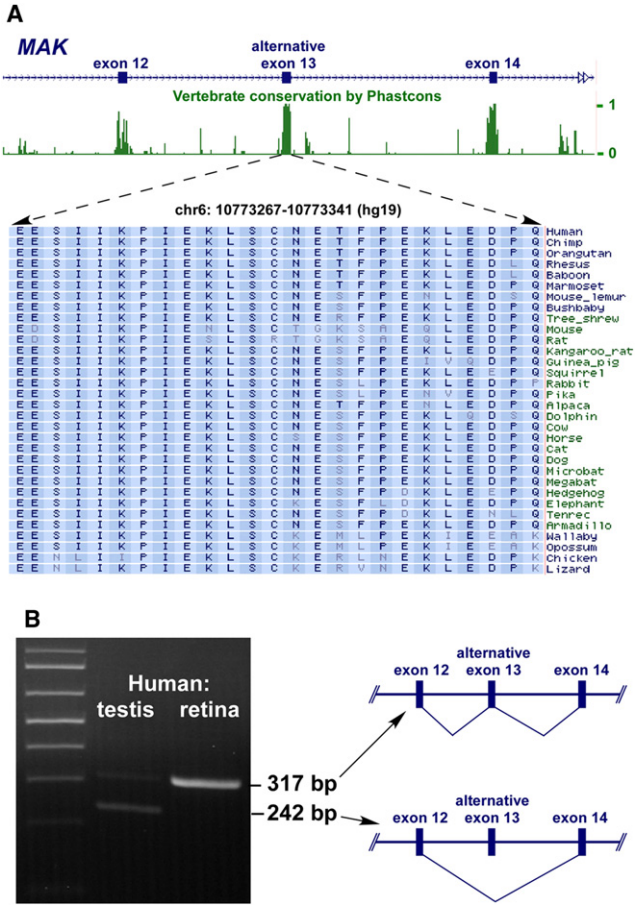

Figure 4. The Predominant Retinal Transcript Isoform of *MAK* Includes an Alternative Exon

(A) Pattern of phylogenetic conservation within the alternative exon of *MAK*. The images are adapted from the UCSC Genome Browser.[38]

(B) PCR results assessing the presence of the alternative exon in cDNA derived from the human retina and testis.

result in a loss of kinase activity in vitro and suggest a critical role for kinase activity in photoreceptor survival in humans. In addition, a retina-enriched transcript isoform of *MAK* was identified that contains an alternative 13th exon. Because all identified *MAK* mutations are shared by both retinal- and testis-enriched isoforms, it is possible that mutations in this gene could affect spermatogenesis. Overall, the *cis*-regulatory mapping approach should be widely applicable to the prioritization of retinal-disease gene candidates, and the generation of ChIP-seq datasets for other retinal disease relevant cell types such as RPE should allow the further extension of this strategy.

Unlike other approaches for candidate-gene prioritization, *cis*-regulatory mapping does not depend on knowledge of gene expression pattern (i.e., whether a candidate gene is enriched in retina) or the extent of gene annotation. In individuals with dominant retinal disease, the list of candidate mutations in exome data is longer compared to that in recessive disease because a single heterozygous mutation is sufficient to cause disease. CRX-based *cis*-regulatory mapping should therefore be particularly useful in such individuals. Overall, CRX-based *cis*-regulatory mapping appears to be a sensitive and versatile tool for prioritizing retinal-disease genes in many rod- and cone-based diseases.

The ability of CRX ChIP-seq data to facilitate candidate-gene prioritization in retinal disease was recently demonstrated in another study that pinpointed mutations in *FAM161A* (MIM 613596) as a cause of RP.[34] In addition, preliminary analyses suggest that CRX-based *cis*-regulatory mapping is effective at prioritizing retinal-disease candidate genes in mice (data not shown). In order to facilitate the application of this approach to mouse models of retinal disease, we have included *cis*-regulatory mapping datasets for mice in Table S1.

The *cis*-regulatory mapping approach introduced here should, in principle, be applicable to disease gene prioritization in any differentiated cell type. Crx is a terminal selector gene that coordinately regulates a host of different genes required for the differentiation of photoreceptors.[10,11,13,35] Such key regulators are known to be present in many cell types. If the identity of a key regulatory transcription factor is known, the creation of a *cis*-regulatory map with ChIP-seq should therefore permit the application of this strategy to other families of diseases affecting specific cell types. For example, CRX-based *cis*-regulatory mapping failed to identify mutations in genes expressed in RPE, and this suggests that additional ChIP-seq datasets for regulators of RPE gene expression such as OTX2 or MITF might facilitate the identification of such disease genes. Similar considerations apply to a range of other disease-relevant cell types throughout the body.

Despite the fact that the CRX ChIP-seq data used in this study were generated in mice, they proved effective at pinpointing photoreceptor genes in humans. This finding suggests that the high degree of phylogenetic conservation observed at many CRX ChIP-seq peaks is indicative of functional conservation at the level of transcriptional control of gene expression. This result stands in contrast to a recent report that found that there is relatively poor cross-species correlation between ChIP-seq peaks for certain liver transcription factors.[36] It is therefore possible that individual transcription factors differ with respect to the evolutionary rate of turnover of their target binding sites. In the case of CRX, this rate appears to be relatively slow.

Mak knockout mice displayed normal retinogenesis, with progressive retinal degeneration of both rods and cones beginning around 1 month of age.[17] This time course of disease progression appears to be somewhat accelerated relative to the human subjects who had *MAK* mutations and whose symptoms first developed relatively late in life. Whereas the visual field defects were a prominent feature in the human subjects, loss of visual acuity was generally mild. Sectorial RP was present in two of the subjects with *MAK* mutations and represents a relatively uncommon subtype of RP in which a specific region of the retina appears to be more heavily or even uniquely affected. Determining the extent of this phenotype will

require the identification of a larger number of individuals with *MAK* mutations.

All of the MAK mutations identified in the present study fall within exons shared by both retinal- and testis-enriched transcript isoforms, raising the possibility that these mutations could have an effect on spermatogenesis. However, there were no reports of infertility in the two male subjects we identified. This finding is consistent with the phenotype of the *Mak* knockout mouse, which is fertile and has only mild defects in sperm motility.[37] Nevertheless, given the expression pattern of *MAK*, analysis of sperm function in subjects carrying mutations in this gene might be warranted.

In conclusion, this study introduces a bioinformatic strategy for prioritizing retinal-disease gene candidates based on the genome-wide pattern of binding of the photoreceptor transcription factor CRX. This approach successfully identified RP-causing mutations in a ciliary gene, *MAK*, and should be widely applicable to retinal-disease gene candidate prioritization in a range of retinal diseases.

Supplemental Data

Supplemental Data include two figures and five tables and can be found with this article online at http://www.cell.com/AJHG/.

Acknowledgements

We sincerely thank all of the families that participated in this study. We also would like to thank Bill Harbour, Mohammed Hussaini, Serkan Kaygın, Lütfiye Mesci, and Atilla Göknur. The European Retinal Disease Consortium consists of Carmen Ayuso, Sandro Banfi, Tamar Ben-Yosef, Elfride de Baere, Christian Hamel, Chris Inglehearn, Robert K. Koenekoop, Susanne Kohl, Bart P. Leroy, Carmel Toomes, and Bernd Wissinger. This work was supported by the National Eye Institute (EY018826), the Hope Center for Neurologic Diseases, and the American Health Assistance Foundation to J.C.C.; the Netherlands Organisation for Scientific Research (TOP-grant 40-00812-98-09047) to F.P.M.C. and A.I.d.H.; the Foundation Fighting Blindness USA (grant BR-GE-0510-04890RAD) to A.I.d.H.; the Algemene Nederlandse Vereniging ter Voorkoming van Blindheid, the Gelderse Blinden Stichting, the Landelijke Stichting voor Blinden en Slechtzienden, Retina Nederland, the Stichting Oogfonds Nederland, and the Rotterdamse Vereniging Blindenbelangen to F.P.M.C.; and Hacettepe University Research Fund (801601003) to R.K.Ö. and a grant from the Foundation Fighting Blindness (BR-GE-0510-0490-HUJ) to D.S.

Received: May 17, 2011
Revised: July 6, 2011
Accepted: July 9, 2011
Published online: August 11, 2011

Web Resources

The URLs for data presented herein are as follows:

Online Mendelian Inheritance in Man, http://www.omim.org
RetNet, Retinal Information Network, http://www.sph.uth.tmc.edu/retnet/

References

1. Ng, S.B., Nickerson, D.A., Bamshad, M.J., and Shendure, J. (2010). Massively parallel sequencing and rare disease. Hum. Mol. Genet. *19* (R2), R119–R124.
2. Ng, S.B., Bigham, A.W., Buckingham, K.J., Hannibal, M.C., McMillin, M.J., Gildersleeve, H.I., Beck, A.E., Tabor, H.K., Cooper, G.M., Mefford, H.C., et al. (2010). Exome sequencing identifies MLL2 mutations as a cause of Kabuki syndrome. Nat. Genet. *42*, 790–793.
3. Ng, S.B., Buckingham, K.J., Lee, C., Bigham, A.W., Tabor, H.K., Dent, K.M., Huff, C.D., Shannon, P.T., Jabs, E.W., Nickerson, D.A., et al. (2010). Exome sequencing identifies the cause of a mendelian disorder. Nat. Genet. *42*, 30–35.
4. Rehman, A.U., Morell, R.J., Belyantseva, I.A., Khan, S.Y., Boger, E.T., Shahzad, M., Ahmed, Z.M., Riazuddin, S., Khan, S.N., Riazuddin, S., and Friedman, T.B. (2010). Targeted capture and next-generation sequencing identifies C9orf75, encoding taperin, as the mutated gene in nonsyndromic deafness DFNB79. Am. J. Hum. Genet. *86*, 378–388.
5. Roach, J.C., Glusman, G., Smit, A.F., Huff, C.D., Hubley, R., Shannon, P.T., Rowen, L., Pant, K.P., Goodman, N., Bamshad, M., et al. (2010). Analysis of genetic inheritance in a family quartet by whole-genome sequencing. Science *328*, 636–639.
6. Rattner, A., Sun, H., and Nathans, J. (1999). Molecular genetics of human retinal disease. Annu. Rev. Genet. *33*, 89–131.
7. den Hollander, A.I., Black, A., Bennett, J., and Cremers, F.P. (2010). Lighting a candle in the dark: Advances in genetics and gene therapy of recessive retinal dystrophies. J. Clin. Invest. *120*, 3042–3053.
8. Daiger, S.P. (2004). Identifying retinal disease genes: How far have we come, how far do we have to go? Novartis Found. Symp. *255*, 17–27, discussion 27–36, 177–178.
9. Corbo, J.C., Lawrence, K.A., Karlstetter, M., Myers, C.A., Abdelaziz, M., Dirkes, W., Weigelt, K., Seifert, M., Benes, V., Fritsche, L.G., et al. (2010). CRX ChIP-seq reveals the cis-regulatory architecture of mouse photoreceptors. Genome Res. *20*, 1512–1525.
10. Livesey, F.J., Furukawa, T., Steffen, M.A., Church, G.M., and Cepko, C.L. (2000). Microarray analysis of the transcriptional network controlled by the photoreceptor homeobox gene Crx. Curr. Biol. *10*, 301–310.
11. Blackshaw, S., Fraioli, R.E., Furukawa, T., and Cepko, C.L. (2001). Comprehensive analysis of photoreceptor gene expression and the identification of candidate retinal disease genes. Cell *107*, 579–589.
12. Furukawa, T., Morrow, E.M., Li, T., Davis, F.C., and Cepko, C.L. (1999). Retinopathy and attenuated circadian entrainment in Crx-deficient mice. Nat. Genet. *23*, 466–470.
13. Hsiau, T.H., Diaconu, C., Myers, C.A., Lee, J., Cepko, C.L., and Corbo, J.C. (2007). The cis-regulatory logic of the mammalian photoreceptor transcriptional network. PLoS ONE *2*, e643.
14. Blackshaw, S., Harpavat, S., Trimarchi, J., Cai, L., Huang, H., Kuo, W.P., Weber, G., Lee, K., Fraioli, R.E., Cho, S.H., et al. (2004). Genomic analysis of mouse retinal development. PLoS Biol. *2*, E247.
15. Bengs, F., Scholz, A., Kuhn, D., and Wiese, M. (2005). LmxMPK9, a mitogen-activated protein kinase homologue affects flagellar length in Leishmania mexicana. Mol. Microbiol. *55*, 1606–1615.
16. Berman, S.A., Wilson, N.F., Haas, N.A., and Lefebvre, P.A. (2003). A novel MAP kinase regulates flagellar length in Chlamydomonas. Curr. Biol. *13*, 1145–1149.

17. Omori, Y., Chaya, T., Katoh, K., Kajimura, N., Sato, S., Muraoka, K., Ueno, S., Koyasu, T., Kondo, M., and Furukawa, T. (2010). Negative regulation of ciliary length by ciliary male germ cell-associated kinase (Mak) is required for retinal photoreceptor survival. Proc. Natl. Acad. Sci. USA *107*, 22671–22676.
18. Hinrichs, A.S., Karolchik, D., Baertsch, R., Barber, G.P., Bejerano, G., Clawson, H., Diekhans, M., Furey, T.S., Harte, R.A., Hsu, F., et al. (2006). The UCSC Genome Browser Database: Update 2006. Nucleic Acids Res. *34* (Database issue), D590–D598.
19. Miller, S.A., Dykes, D.D., and Polesky, H.F. (1988). A simple salting out procedure for extracting DNA from human nucleated cells. Nucleic Acids Res. *16*, 1215.
20. Collin, R.W., van den Born, L.I., Klevering, B.J., de Castro-Miró, M., Littink, K.W., Arimadyo, K., Azam, M., Yazar, V., Zonneveld, M.N., Paun, C.C., et al. (2011). High-resolution homozygosity mapping is a powerful tool to detect novel mutations causative of autosomal recessive RP in the Dutch population. Invest. Ophthalmol. Vis. Sci. *52*, 2227–2239.
21. Purcell, S., Neale, B., Todd-Brown, K., Thomas, L., Ferreira, M.A., Bender, D., Maller, J., Sklar, P., de Bakker, P.I., Daly, M.J., and Sham, P.C. (2007). PLINK: A tool set for whole-genome association and population-based linkage analyses. Am. J. Hum. Genet. *81*, 559–575.
22. Liu, Q., Tan, G., Levenkova, N., Li, T., Pugh, E.N., Jr., Rux, J.J., Speicher, D.W., and Pierce, E.A. (2007). The proteome of the mouse photoreceptor sensory cilium complex. Mol. Cell. Proteomics *6*, 1299–1317.
23. Dryja, T.P., McGee, T.L., Reichel, E., Hahn, L.B., Cowley, G.S., Yandell, D.W., Sandberg, M.A., and Berson, E.L. (1990). A point mutation of the rhodopsin gene in one form of retinitis pigmentosa. Nature *343*, 364–366.
24. Rosenfeld, P.J., Cowley, G.S., McGee, T.L., Sandberg, M.A., Berson, E.L., and Dryja, T.P. (1992). A null mutation in the rhodopsin gene causes rod photoreceptor dysfunction and autosomal recessive retinitis pigmentosa. Nat. Genet. *1*, 209–213.
25. Azam, M., Collin, R.W., Shah, S.T., Shah, A.A., Khan, M.I., Hussain, A., Sadeque, A., Strom, T.M., Thiadens, A.A., Roosing, S., et al. (2010). Novel CNGA3 and CNGB3 mutations in two Pakistani families with achromatopsia. Mol. Vis. *16*, 774–781.
26. Corbo, J.C., Myers, C.A., Lawrence, K.A., Jadhav, A.P., and Cepko, C.L. (2007). A typology of photoreceptor gene expression patterns in the mouse. Proc. Natl. Acad. Sci. USA *104*, 12069–12074.
27. Mears, A.J., Kondo, M., Swain, P.K., Takada, Y., Bush, R.A., Saunders, T.L., Sieving, P.A., and Swaroop, A. (2001). Nrl is required for rod photoreceptor development. Nat. Genet. *29*, 447–452.
28. Daniele, L.L., Lillo, C., Lyubarsky, A.L., Nikonov, S.S., Philp, N., Mears, A.J., Swaroop, A., Williams, D.S., and Pugh, E.N., Jr. (2005). Cone-like morphological, molecular, and electrophysiological features of the photoreceptors of the Nrl knockout mouse. Invest. Ophthalmol. Vis. Sci. *46*, 2156–2167.
29. Burghoorn, J., Dekkers, M.P., Rademakers, S., de Jong, T., Willemsen, R., and Jansen, G. (2007). Mutation of the MAP kinase DYF-5 affects docking and undocking of kinesin-2 motors and reduces their speed in the cilia of Caenorhabditis elegans. Proc. Natl. Acad. Sci. USA *104*, 7157–7162.
30. Hanks, S.K., and Hunter, T. (1995). Protein kinases 6. The eukaryotic protein kinase superfamily: Kinase (catalytic) domain structure and classification. FASEB J. *9*, 576–596.
31. Taylor, S.S., Zheng, J., Radzio-Andzelm, E., Knighton, D.R., Ten Eyck, L.F., Sowadski, J.M., Herberg, F.W., and Yonemoto, W.M. (1993). cAMP-dependent protein kinase defines a family of enzymes. Philos. Trans. R. Soc. Lond. B Biol. Sci. *340*, 315–324.
32. Taylor, S.S., Knighton, D.R., Zheng, J., Ten Eyck, L.F., and Sowadski, J.M. (1992). Structural framework for the protein kinase family. Annu. Rev. Cell Biol. *8*, 429–462.
33. Thomas, J., Morlé, L., Soulavie, F., Laurençon, A., Sagnol, S., and Durand, B. (2010). Transcriptional control of genes involved in ciliogenesis: A first step in making cilia. Biol. Cell *102*, 499–513.
34. Langmann, T., Di Gioia, S.A., Rau, I., Stöhr, H., Maksimovic, N.S., Corbo, J.C., Renner, A.B., Zrenner, E., Kumaramanickavel, G., Karlstetter, M., et al. (2010). Nonsense mutations in FAM161A cause RP28-associated recessive retinitis pigmentosa. Am. J. Hum. Genet. *87*, 376–381.
35. Hobert, O. (2008). Regulatory logic of neuronal diversity: Terminal selector genes and selector motifs. Proc. Natl. Acad. Sci. USA *105*, 20067–20071.
36. Schmidt, D., Wilson, M.D., Ballester, B., Schwalie, P.C., Brown, G.D., Marshall, A., Kutter, C., Watt, S., Martinez-Jimenez, C.P., Mackay, S., et al. (2010). Five-vertebrate ChIP-seq reveals the evolutionary dynamics of transcription factor binding. Science *328*, 1036–1040.
37. Shinkai, Y., Satoh, H., Takeda, N., Fukuda, M., Chiba, E., Kato, T., Kuramochi, T., and Araki, Y. (2002). A testicular germ cell-associated serine-threonine kinase, MAK, is dispensable for sperm formation. Mol. Cell. Biol. *22*, 3276–3280.
38. Kuhn, R.M., Karolchik, D., Zweig, A.S., Wang, T., Smith, K.E., Rosenbloom, K.R., Rhead, B., Raney, B.J., Pohl, A., Pheasant, M., et al. (2009). The UCSC Genome Browser Database: update 2009. Nucleic Acids Res. *37* (Database issue), D755–D761.